



## Nonnegligible role of biomass types and its compositions on the formation of persistent free radicals in biochar: Insight into the influences on Fenton-like process

Danlian Huang<sup>a,b,\*</sup>, Hao Luo<sup>a,b</sup>, Chen Zhang<sup>a,b,\*</sup>, Guangming Zeng<sup>a,b</sup>, Cui Lai<sup>a,b</sup>, Min Cheng<sup>a,b</sup>, Rongzhong Wang<sup>a,b</sup>, Rui Deng<sup>a,b</sup>, Wenjing Xue<sup>a,b</sup>, Xiaomin Gong<sup>a,b</sup>, Xueying Guo<sup>a,b</sup>, Tao Li<sup>a,b</sup>

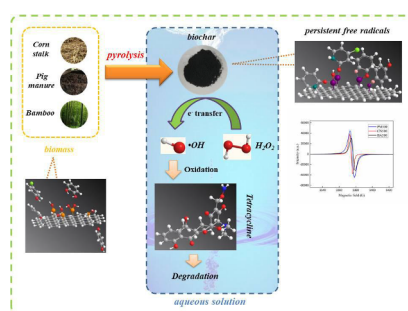
<sup>a</sup> College of Environmental Science and Engineering, Hunan University, Changsha 410082, People's Republic of China

<sup>b</sup> Key Laboratory of Environmental Biology and Pollution Control (Hunan University), Ministry of Education, Changsha 410082, People's Republic of China

### HIGHLIGHTS

- Three types of biochar can efficiently activate hydrogen peroxide.
- Biochar/H<sub>2</sub>O<sub>2</sub> systems exhibited high tetracycline degradation efficiency.
- Catalytic property of biochar depends on the amounts of PFRs.
- Biomass types and its compositions were crucial for the formation of PFRs.
- Electron transfer pathways could be the catalytic mechanisms of biochar.

### GRAPHICAL ABSTRACT



### ARTICLE INFO

#### Keywords:

Heterogeneous Fenton-like systems  
Persistent free radicals  
Biomass  
Biochar/H<sub>2</sub>O<sub>2</sub> systems  
Degradation

### ABSTRACT

Biochar, a green material that possesses high catalytic potential due to its persistent free radicals (PFRs), has attracted increasing attention in the removal of refractory pollutants from water. The influences of biomass types (bamboo, corn stalk, and pig manure) and its compositions (metals and phenolic compounds) on the formation of PFRs in biochar were investigated by electron paramagnetic resonance (EPR). It was found that the amounts of PFRs in biochar would decrease sharply with the decrease of the initial metals and phenolic compounds existed in biomass, and the effect of metals contents on PFRs formation was much greater than that of phenolic compounds contents. This finding was supported by the results obtained from elemental analysis and molar H/C analysis of three types of biochar, which suggested that pig-manure biochar (PM500) had the highest concentrations of PFRs of  $14.13 \times 10^{18}$  spins·g<sup>-1</sup> due to the high content of metals and phenolic compounds in pig manure. The EPR trapping experiment and Linear sweep voltammetry (LSV) measurements in biochar/H<sub>2</sub>O<sub>2</sub> systems showed that ·OH was the dominant reactive radical and electrons transfer pathways might be responsible for the activation of H<sub>2</sub>O<sub>2</sub> by biochar. Possible degradation pathways of the tetracycline in biochar/H<sub>2</sub>O<sub>2</sub> systems were also proposed. Besides, high degradation efficiency and good stability were observed in real wastewater application of the PM500/H<sub>2</sub>O<sub>2</sub> system. These findings would provide a clearer insight into the formation mechanisms of PFRs in biochar, and also present a better strategy for biochar preparation and application in Fenton-like system.

\* Corresponding authors at: College of Environmental Science and Engineering, Hunan University, Changsha 410082, People's Republic of China.  
E-mail addresses: [huangdanlian@hnu.edu.cn](mailto:huangdanlian@hnu.edu.cn) (D. Huang), [zhangchen@hnu.edu.cn](mailto:zhangchen@hnu.edu.cn) (C. Zhang).

<https://doi.org/10.1016/j.cej.2018.12.098>

Received 6 August 2018; Received in revised form 26 November 2018; Accepted 18 December 2018

Available online 19 December 2018

1385-8947/ © 2018 Published by Elsevier B.V.

## 1. Introduction

Persistent organic pollutants, like antibiotics, have caused a number of ecological problems in the aquatic environment. Finding an efficient and practical method to remove refractory pollutants from water has become a focused issue. Advanced oxidation processes (AOPs), especially Fenton/Fenton-like reaction, are widely used to deal with the persistent organic pollutants in water owing to its simple operation, eco-friendly and high treatment efficiency [1–4]. The essence of the traditional Fenton method is that  $\text{Fe}^{2+}$  can act as a catalyst to activate the transformation of hydrogen peroxide ( $\text{H}_2\text{O}_2$ ) to hydroxyl radical ( $\cdot\text{OH}$ ), but this process is accompanied with the production of large amount of sludges and the leaching of metal ions which might result in secondary pollution [5–8]. There were a lot of efforts to improve the Fenton method that made by the previous studies [9–12]. Our team found that the novel synthesized material steel converter slag modified by salicylic acid-methanol and cobalt nitrate (Co-SAM-SCS) can remarkably promote the activation of  $\text{H}_2\text{O}_2$  due to the synergistic effect between introduced Co and SAM-SCS [13]. Chen and co-workers found that the  $\text{CeO}_2$  modified with sulfate groups as acidic sites or pretreated by sulfation can significantly improve the catalytic activity of  $\text{CeO}_2/\text{H}_2\text{O}_2$  system [14,15]. Although these novel compound materials possesses excellent catalytic properties, there is an inevitable fact that the problem of metal leaching still exists and the limited raw materials may cause a higher fabricating cost due to the multi-step productive process. Therefore, it is particularly important to find an environmental-friendly catalyst with satisfactory performance.

Pyrogenic carbonaceous matter, including biochar, activated carbon, and related materials like graphene and nanotubes, have been used in Fenton/Fenton-like systems to replace iron catalysts due to their great superiorities in well-developed pore structure, large surface area and highly active surface functional groups. Nilsun H. Ince and Izzet G. Apikyan [16] have discovered that activated carbon can efficiently degrade phenol by catalyze  $\text{H}_2\text{O}_2$ . After that, researchers constantly found that many porous carbon materials (graphite carbon, mesoporous carbon, and activated carbon fiber, etc.) can be used as the support of catalyst, sometimes even as a direct catalyst, to participate in the activation process of peroxide oxidants ( $\text{H}_2\text{O}_2$ , persulfate, and peracetic acid, etc.) [17–23]. These activation processes could produce strongly oxidized free radicals ( $\cdot\text{OH}$ , sulfate radical, and alkoxy radicals, etc.) which can effectively degrade persistent organic pollutants in water environment. Compared with other carbon materials, biochar, a sustainable pyrolysis product of agricultural solid waste, has attracted extensively attention in the application of catalysis as its low cost, simple preparation, and higher reactive surface composition [24–28]. It has been reported that biochar has the ability to transfer electrons due to the existence of persistent free radicals (PFRs) so that it can activate  $\text{H}_2\text{O}_2$  or persulfate to remove refractory organic pollutants [29,30]. PFRs may be the saturated free radical product formed by the combination of the carbon-centric dangling bond and the molecular oxygen during the process of natural cooling of the freshly prepared biochar [31–33]. It was also reported that a portion of these saturated free radical products would fade away in a few hours and the other part could exist a long time due to the widely  $\pi$ -delocalization function or the separation with the surface of material [34,35]. A preliminarily work studied the influence of the morphological structure and chemical characteristics of the wheat stalk biochar on  $\text{H}_2\text{O}_2$  activation, the results showed that the big porous structure and high aromatic degree of the high temperature biochar were advantageous to the generation of  $\cdot\text{OH}$  [36]. Vejerano E and his group found that PFRs may be formed through the thermolysis of peculiar organic molecular (phenols, catechols, and hydroquinones, etc.) chemisorbed by metal oxides and this process followed a mechanism of electron transfer from the adsorbate to the metal atom [37–40]. Therefore, it is hypothesized that the formation of PFRs in biochar may follow a similar mechanism. However, there is a crucial but almost neglected issue that the different types and

compositions of feedstocks will change the properties of biochar, which can affect the formation of PFRs in biochar [41–44]. Hence, the study about the effects of biomass types and its compositions on the PFRs in biochar can better explain the formation mechanisms of PFRs.

The main objectives of this paper were as follows: (1) To demonstrate the relationship between the PFRs in biochar and the catalytic ability of biochar in Fenton-like systems; (2) To understand the influences of different compositions of biomass on the formation of PFRs in biochar by changing the ingredients in the feedstocks; (3) To explore the possible catalytic mechanisms of biochar in biochar/ $\text{H}_2\text{O}_2$  systems and the formation mechanisms of PFRs in biochar. Considering the harmful effects on ecology environment and human health, tetracycline (TC) was selected as the model contaminant to evaluate the degradation efficiency of biochar/ $\text{H}_2\text{O}_2$  system and the mechanism of TC degradation by  $\cdot\text{OH}$  was also investigated [45,46].

## 2. Materials and methods

### 2.1. Materials

Three types of common biomass including corn stalks (CN), bamboo (BA), and pig manure (PM) were collected from villages of Changsha, Hunan province, China. TC was obtained from Sigma Chemical Company (99%, w/w).  $\text{H}_2\text{O}_2$  (30%) was purchased from J&K Scientific Ltd, China. Glycerol, EDTA and the rest of the chemicals were purchased from China National Medicines Corporation Ltd (Beijing, China), ultra-pure water (resistivity of 18.25  $\text{M}\Omega\text{cm}$ ) was used throughout the experiments.

### 2.2. Metals and phenolic compounds extraction experiment

To change the contents of metals and phenolic compounds in feedstock, three types of biomass (CN, BA, and PM) was extracted by 120 mM EDTA and 40 mM Glycerol, correspondingly. Firstly, biomass materials were rinsed with ultra-pure water three times to remove dust particles and dried at 60 °C for 24 h, the oven-dried biomass materials were ground into powder by a high-speed rotary pulverizer and screened through a 100-mesh sieve. Then, 800 mg of these samples powders was added to 100 mL aqueous solution containing an extracting agent. After being shaken for a definite period in a stoppered centrifuge tube at room temperature (25 °C), the samples were filtered and collected, while the rest of solution was analyzed by high performance liquid chromatography (Agilent 1100, America) and Atomic Absorption Spectrometry (Z-2000, Hitachi, Japan). The obtained samples were rinsed with ultra-pure water three times to remove extracting agent and dried at 60 °C for 24 h. After that, these samples were stored in an anaerobic glovebox purged with  $\text{N}_2$  for future use.

### 2.3. Biochar preparation

All the biomass materials used in this study were rinsed with ultra-pure water three times to remove dust particles and dried at 60 °C for 24 h, then the oven-dried biomass materials were ground into powder by a high-speed rotary pulverizer and screened through a 100-mesh sieve. The pyrolysis processes were as follows: Firstly, the dried biomass powders were put in a quartz boat and pyrolysed with  $\text{N}_2$  purge ( $0.5\text{L}\cdot\text{min}^{-1}$ ) at a heating rate of  $8\text{ }^\circ\text{C}\cdot\text{min}^{-1}$  in a tube furnace, then all the biomass materials were processed using a temperature programming method (pyrolysed for 2 h at temperatures of 500 °C). The obtained biochar were ground to below 0.15 mm and stored in an anaerobic glovebox purged with  $\text{N}_2$  to avoid the effects of oxygen molecule on the PFRs concentrations contained in biochar.

### 2.4. Degradation experiments

A series of degradation experiments were performed in 100 mL

conical flasks consisting of 40 mL of reaction solution. Firstly, 20 mg biochar was put into 39 mL aqueous solution of tetracycline (67.5  $\mu\text{M}$ ) at pH 7.4 (20 mM phosphate buffer) at 25 °C. After complete mixing, 1.0 mL of 0.2 M  $\text{H}_2\text{O}_2$  (the final concentration was 5 mM) was promptly added to start the reaction, and the mixtures were kept shaking at 150 rpm and 25 °C in constant temperature bath oscillator (SHZ-88, China) for different reaction times. The control experiments without  $\text{H}_2\text{O}_2$  or biochar were conducted under the same reaction conditions. At regular intervals, a fraction of samples were sacrificed for analysis and filtered through 0.22  $\mu\text{m}$  nylon membranes, and 1.0 mL of ethanol was added into 3.0 mL solution to stop the reaction. The concentration of tetracycline was analyzed by an ultraviolet spectrophotometer (UV-2600, Japan). The filtered biochar particles were collected and freeze-dried by vacuum freeze dryer (Biosafer-10A, China), and then measured by Electron Paramagnetic Resonance (EPR) to quantify the intensity of its PFRs after reaction. To quantify the adsorption capacity of tetracycline by biochar, the filtered biochar particles were also extracted by ethylene glycol, and the recovery rate of TC was investigated. The remaining solution after reaction was filtered through 0.22  $\mu\text{m}$  nylon membranes and then analyzed by Atomic Absorption Spectrometry (Z-2000, Hitachi, Japan) to detect the concentration of metals released from surface of biochar.

### 2.5. EPR measurements

The EPR spectra of biochar samples before and after catalysis reaction were obtained at 25 °C by a MS5000 (Germany), with a resonance frequency of 9.45 GHz, microwave power of 27 mW, modulation frequency of 100 kHz, modulation amplitude of 2.0 G, sweep width of 100 G, a time constant of 98.22 ms, and a sweep time of 60.00 s. The PFRs concentration contained in biochar was quantified by EPR using an MgO standard sample tube doped with  $1.01 \times 10^{15} \text{Cr}^{3+}/\text{cm}^3$ . The peak-to-peak width ( $\Delta H_{p-p}$ ) g-factor and g-factor of the EPR spectra were obtained by simulating the EPR spectra with EPRstudio (Germany).

The generation of  $\cdot\text{OH}$  from biochar/ $\text{H}_2\text{O}_2$  suspensions was investigated by EPR spectroscopy coupled with 5, 5-dimethyl-1-pyrroline N-oxide (DMPO) as the spin-trapping agent. First, 20 mg biochar was thoroughly mixed with 40 mL  $\text{H}_2\text{O}_2$  (5 mM) solution at pH 7.4 (20 mM phosphate buffer, 25 °C) and 2 mL of reaction solution was sampled at different time points as the reaction progressed. Then, 1 mL of 0.2 M DMPO was added into these reaction solutions immediately. After sufficient reaction, these mixtures were filtered through 0.22  $\mu\text{m}$  nylon membranes and analyzed by EPR spectrometer. An aliquot of 5 mM Potassium dichromate ( $\text{K}_2\text{Cr}_2\text{O}_7$ ) would also be added to the mixed biochar/ $\text{H}_2\text{O}_2$  system under identical conditions to explore the catalytic mechanism of biochar for  $\text{H}_2\text{O}_2$  activation. The EPR spectra were obtained at 25 °C by a MS5000 (Germany), with a resonance frequency of 9.45 GHz, microwave power of 27 mW, modulation frequency of 100 kHz, modulation amplitude of 2.0 G, sweep width of 100 G, a time constant of 98.22 ms, and a sweep time of 60.00 s. Peak intensities of DMPO-OH were used as an index of the concentrations of  $\cdot\text{OH}$  and were measured by EPRstudio (Germany).

### 2.6. Characterization methods

An elemental analyzer (model EA1110, CE Instruments, Milan, Italy) was used to analyze the elemental compositions (C, H, N, and O) of samples. And the extractable metals (Ca, Mg, Fe, Zn, and Mn) of samples were determined by Atomic Absorption Spectrometry (Z-2000, Hitachi, Japan) following the acid digestion. In this process, (a) a mixture of 5 mL  $\text{HNO}_3$ , 5 mL HF and 3 mL  $\text{HClO}_4$  were added into 20 mg biochar, (b) Hotblock: 90 °C for 40 mins, 140 °C for 60 mins, 170 °C for 40 mins, (c) diluted the products with ultrapure water to a volume of 100 mL [47,48]. The chemical indicators (COD,  $\text{NH}_3\text{-N}$ , TP, and TN) of real water used in this study were analyzed by automatic determinator

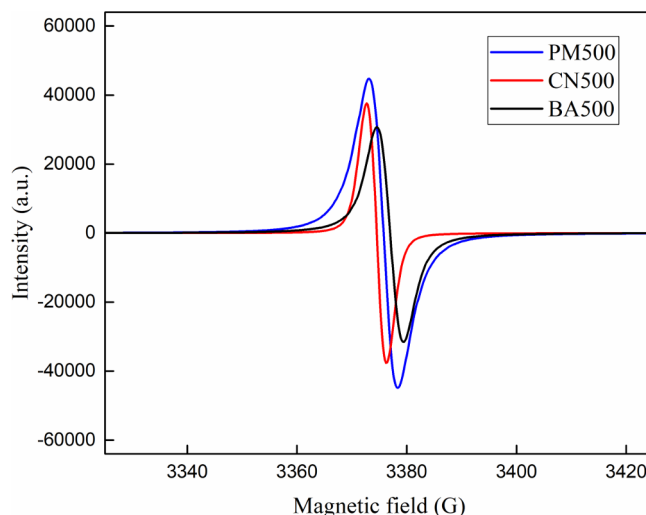


Fig. 1. EPR spectra of biochar particles pyrolysed from three types of biomass (pig manure, corn stalk and bamboo) at 500 °C for 2 h. Experimental conditions: samples quality: PM500 = 20 mg, CN500 = 20 mg, BA500 = 20 mg; T = 25 °C.

(TR-408, China) while metals (Cd and Pb) in these water were also determined by Atomic Absorption Spectrometry (Z-2000, Hitachi, Japan).

In order to make the experimental data more accurate and reliable, three parallel samples were prepared for each set of experiments and each test was repeated for three times. All data would calculate standard deviation and standard error of the sample. If the deviation was too large, it would be resampled until the deviation reaches a reasonable range. Then, the arithmetic mean value of the sample data will be used as the basis of subsequent experimental analysis, and the error bar will be indicated in the graph through the confidence interval calculated by standard error.

## 3. Results and discussion

### 3.1. Effects of feedstocks on PFRs in biochar

The effects of the biomass types on the PFRs in biochar were analyzed by EPR spectroscopy. According to Fig. 1, there can be observed a broad singlet EPR signal in three different biochar (derived from CN, BA, PM) pyrolysed at 500 °C for 2 h, while no EPR signal could be seen in these biomass without pyrolysis. These spectrograms were similar with the EPR signals observed in pine needle-derived biochar according to previous studies [29,30]. The g-factors and  $\Delta H_{p-p}$  were 2.0046 and 6.9 G for BA500, 2.0049 and 6.2 G for CN500, 2.0048 and 7.0 G for PM500 (Table S1). Previous studies reported that the g-factors for semiquinone radicals were larger than 2.0045, those for oxygen-centered radicals were larger than 2.0040; while carbon-centered radicals with an adjacent oxygen atom had g-factors in the range of 2.0030–2.0040, and carbon-centered had g-factors less than 2.0030 [29,38]. The results observed in this study suggested that PFRs formed in three types of biochar are representative oxygen-centered free radicals where the unpaired electron is located on an oxygen atom. Similar conclusions also can be found in previous papers which the g-factors ranged from 2.0028 to 2.0037 with  $\Delta H_{p-p}$  of 4.5–6.8 G indicating that all of these PFRs formed in pine needles biochar are carbon-centered radicals or carbon-centered radicals with adjacent oxygen atom [29,30]. The concentration of PFRs determined by EPR spectroscopy on three different type of biochar were  $7.94 \times 10^{18} \text{spins}\cdot\text{g}^{-1}$  for BA500,  $9.67 \times 10^{18} \text{spins}\cdot\text{g}^{-1}$  for CN500 and  $14.13 \times 10^{18} \text{spins}\cdot\text{g}^{-1}$  for PM500, respectively. These results indicated that biomass type has a significant effect on the formation of PFRs in biochar.

Previous studies found that organic constituents may have a

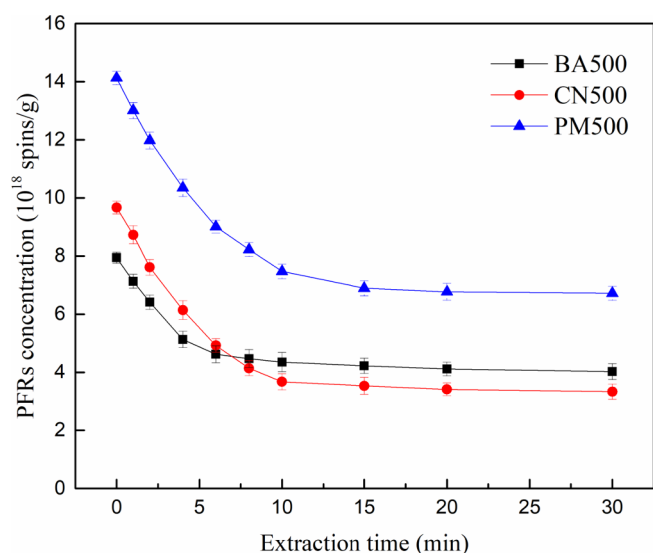


**Fig. 2.** Changes of PFRs concentration in biochar pyrolysed from the biomass that extracted by Glycerol with different extraction time. Experimental conditions: [PM] = 8 g/L; [CN] = 8 g/L; [BA] = 8 g/L; [Glycerol] = 40 mM; T = 25 °C.

significant influence on the formation of PFRs [49,50]. Organic compounds such as phenolic compounds in biomass could be the crucial factor to control the formation of PFRs in biochar, and phenolic compounds were precursors of PFRs production [29,51–53]. Furthermore, it was found that PFRs can act as an electron shuttle to mediate the reduction of metal ions [54–56]. There are some reports revealed that metals in biomass also contributed to the formation of PFRs in biochar [30,51]. Hence, we presumed that the diversity about the contents of organic compounds and metals in biomass may cause the difference of the amounts of PFRs formed in the biochar produced from these materials, and the following experiment is to demonstrate it.

It has been reported that organic compounds, especially phenolic compounds, in biomass would participate in the formation of PFRs in biochar [30,51,57]. Glycerol is an efficient solvent to extract phenolic compounds from biomass and will extract more amounts of phenolic compounds with the longer extraction time [58]. Therefore, to further demonstrate the role of phenolic compounds on the formation of PFRs, three types of biomass were extracted by Glycerol with different extraction time, and then these materials were used to produce biochar. As shown in Fig. 2, the concentrations of PFRs in biochar decreased rapidly from  $7.94 \times 10^{18}$  spins·g<sup>-1</sup> to  $4.62 \times 10^{18}$  spins·g<sup>-1</sup> for BA500 within 6 min, from  $9.67 \times 10^{18}$  spins·g<sup>-1</sup> to  $3.67 \times 10^{18}$  spins·g<sup>-1</sup> for CN500 within 10 min and from  $14.13 \times 10^{18}$  spins·g<sup>-1</sup> to  $6.89 \times 10^{18}$  spins·g<sup>-1</sup> for PM500 within 15 min, which suggested that the extraction of Phenolic compounds from biomass significantly decreased the formation of PFRs in biochar and pig manure has the highest content of phenolic compounds. At the same time, the elemental compositions of three biochar samples that we determined by an elemental analyzer were also consistent with this result. H/C molar ratios can be analyzed to evaluate the degree of aromaticity of chars, the decrease of H/C value was closely correlated to the formation of higher aromatic ring structures in biochar [59,60], Table S2 showed that the H/C molar ratios were 0.772, 0.695, and 0.606 for BA500, CN500, and PM500, respectively, which means that PM500 has the highest degree of aromaticity. The possible reason for this result could be that most of PFRs converted from the Phenolic compounds in biomass under pyrolysis process may have polyaromatic structures or aromatic subunits [51,61].

EDTA can act as a chelating agent to remove the metals (e.g., Ca, Mg, Cu, Fe, and Zn) from soils or carbon materials [62–64]. To

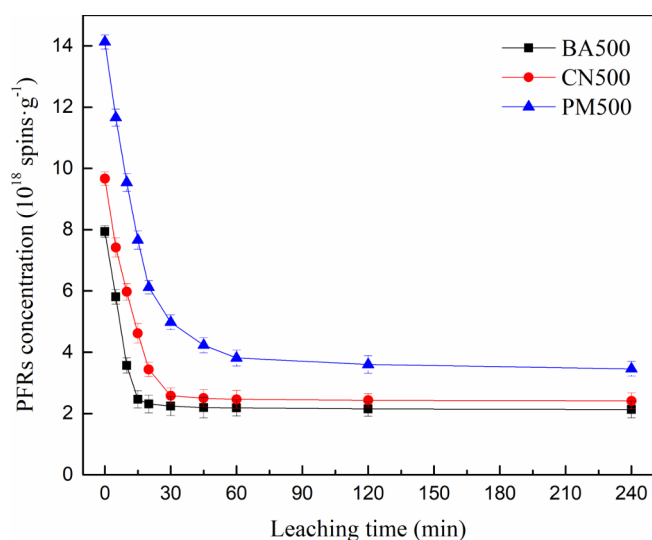
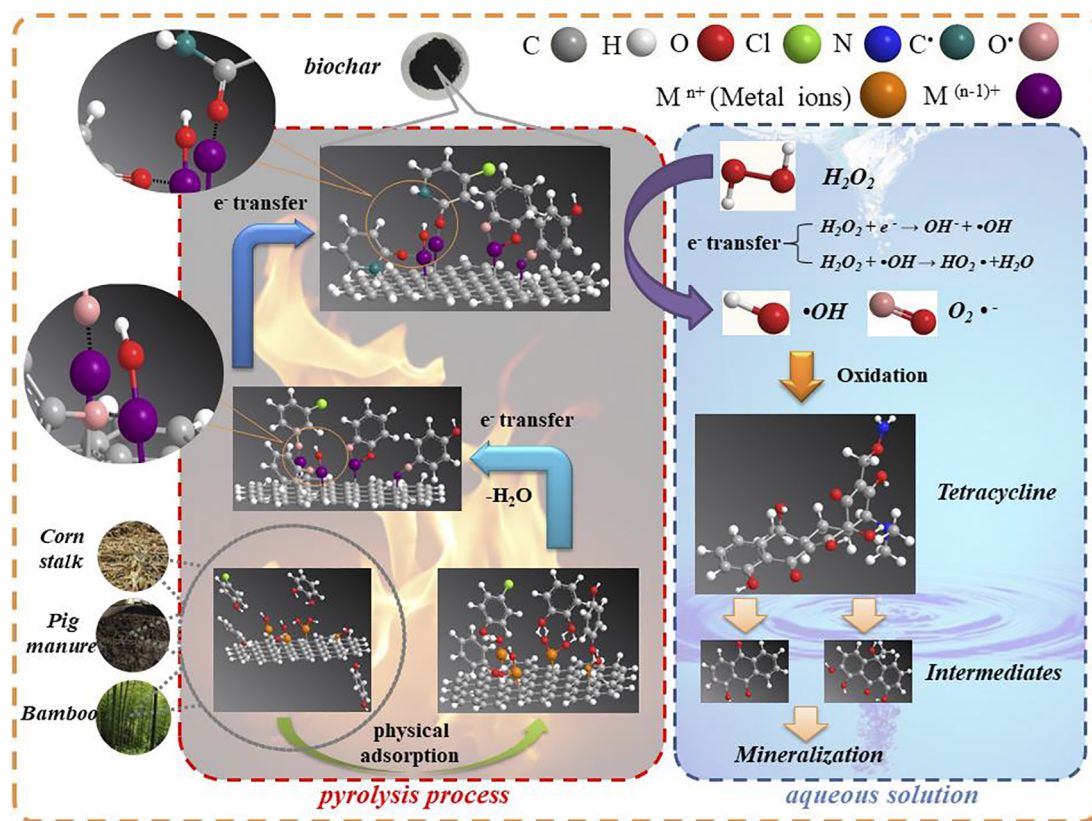


**Fig. 3.** Changes of PFRs concentration in biochar pyrolysed from the biomass that immersed by EDTA with different leaching time. Experimental conditions: [PM] = 8 g/L; [CN] = 8 g/L; [BA] = 8 g/L; [EDTA] = 120 mM; T = 25 °C.

elucidate the function of metals in the formation of PFRs, three type of biomass were immersed in 120 mM EDTA solution, and then used to produce biochar. According to Fig. 3, with the application of EDTA, the concentration of PFRs decreased sharply from  $7.94$  spins·g<sup>-1</sup> to  $2.46$  spins·g<sup>-1</sup> for BA500 within 15 min, from  $9.67$  spins·g<sup>-1</sup> to  $2.58$  spins·g<sup>-1</sup> for CN500 within 30 min, and from  $14.13$  spins·g<sup>-1</sup> to  $3.81$  spins·g<sup>-1</sup> for PM500 within 60 min, which means that the decrease of metals content in biomass result in the remarkable reduction of the concentration of PFRs in biochar. Surprisingly, we found that the decrease degree of the PFRs concentration in biochar produced from the biomass immersed by EDTA is much greater than the biomass extracted by glycerol. To verify this result, the EDTA solution after leaching experiment has been detected by high performance liquid chromatography (HPLC) and there were no obvious peaks of phenolic compounds in the test result. Previous papers found that the PFRs can be formed from organic compounds (e.g., phenols, chlorobenzenes) adsorbed on metal oxide surfaces under combustion conditions through the mechanism of electron transfer from organic compounds to metals [37,39,40]. Therefore, we believe that the possible reason for this result is that metals in the biomass play a vital role in the formation of PFRs in biochar. The main part of PFRs might be a metal-organic combination formed by the combination of organic groups and metal center during the process of the electron transfer from organic compounds to metal oxide. In the process of the formation of PFRs, metals may play a role in accepting electrons and connecting the components of PFRs, while phenolic compounds would lose electrons and become a part of PFRs. It has been reported that PFRs formed in combustion products were stabilized by their interaction with the metal oxide domain surface and thus different metal oxides can influence the half-lives of PFRs due to the different strength of the interaction [65]. The half-lives of PFRs formed on ZnO ranged from 3 to 73 days which were much longer than Fe<sub>2</sub>O<sub>3</sub> (24–111 h) and CuO (27 to 74 min) [37–40]. Hence, the amount of organic compounds in biomass determined the concentration of PFRs in biochar, while metal is a crucial factor in the formation of PFRs. Consequently, the proposed mechanism for the formation of PFRs in biochar from the pyrolysis of biomass was depicted in Scheme 1. Table S2 showed that the metal content of three kinds of biomass measured by Z-2000, while pig manure has the highest total metal content. This result was coincided with the phenomenon suggested in the Fig. 3, which the concentration of PFRs in PM biochar has the biggest decline compared to the other two biochar with the longer leaching time.



Scheme 1. Proposed formation mechanisms of PFRs in biochar and the degradation of TC in biochar/H<sub>2</sub>O<sub>2</sub> system.

### 3.2. Catalytic performances in biochar/H<sub>2</sub>O<sub>2</sub> systems

To further demonstrate the catalytic ability of biochar for H<sub>2</sub>O<sub>2</sub> activation, the degradation of TC was studied. Fig. 4a showed that the degradation efficiency of 30 mg/L TC was 100% for PM500/H<sub>2</sub>O<sub>2</sub>, 96% for CN500/H<sub>2</sub>O<sub>2</sub>, 87% for BA500/H<sub>2</sub>O<sub>2</sub>, 74% for PM500-Glycerol-30 min/H<sub>2</sub>O<sub>2</sub>, and 38% for PM500-EDTA-2 h/H<sub>2</sub>O<sub>2</sub> respectively. Oppositely, only 12.3%, 14.6%, 11.7%, 15.3%, or 17.2% of TC was removed in the corresponding system without H<sub>2</sub>O<sub>2</sub>, which was due to the adsorption in biochar. Besides, less than 23% of TC was degraded in control experiments without biochar. The degradation of TC can be

described by following equation,

$$[TC] = [TC]_0 e^{-k_{obs}t}$$

where  $k_{obs}$  is the pseudo-first-order rate constant,  $[TC]_0$  is the initial concentration of TC, and  $[TC]$  is the concentration of TC at reaction time  $t$ . Hence,  $k_{obs}$  can be calculated through the linear regression of plot of  $\ln([TC]/[TC]_0)$  against time  $t$ . According to Fig. 4b,  $k_{obs}$  were  $0.005 \text{ min}^{-1}$  for PM500-EDTA-2 h/H<sub>2</sub>O<sub>2</sub>,  $0.006 \text{ min}^{-1}$  for PM500-Glycerol-30 min/H<sub>2</sub>O<sub>2</sub>,  $0.008 \text{ min}^{-1}$  for BA500/H<sub>2</sub>O<sub>2</sub>,  $0.011 \text{ min}^{-1}$  for CN500/H<sub>2</sub>O<sub>2</sub>,  $0.021 \text{ min}^{-1}$  for PM500/H<sub>2</sub>O<sub>2</sub>, respectively. These results indicated that the biochar/H<sub>2</sub>O<sub>2</sub> systems can efficiently degraded

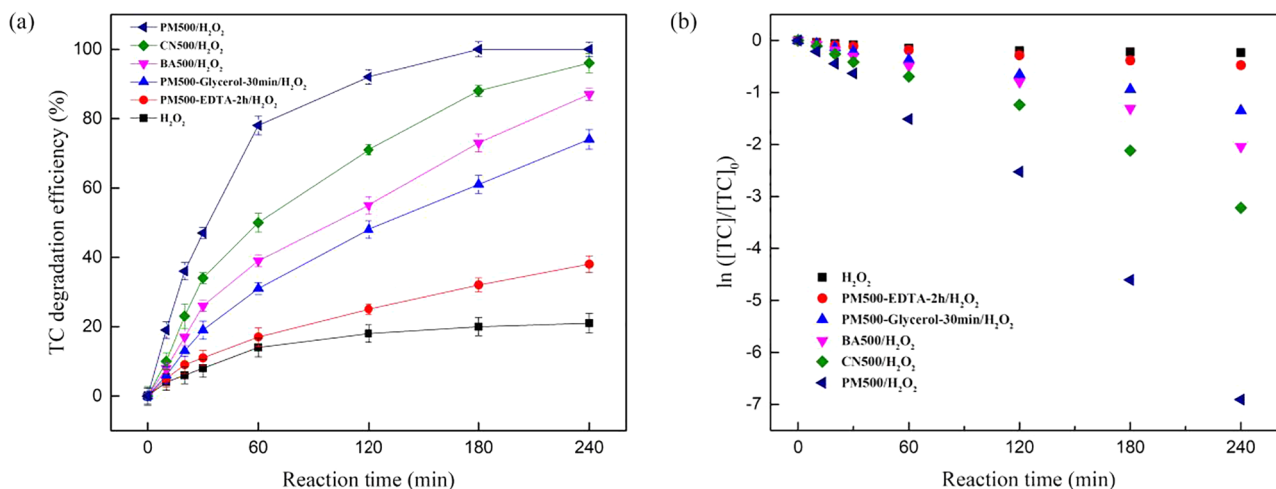


Fig. 4. Degradation efficiency of TC (a) and pseudo first-order fitting for TC degradation (b) in the different biochar/H<sub>2</sub>O<sub>2</sub> systems. Reaction conditions:  $[H_2O_2]_0 = 5 \text{ mM}$ ;  $[TC]_0 = 67.5 \text{ } \mu\text{M}$ ;  $[PM500] = 0.5 \text{ g/L}$ ;  $[CN500] = 0.5 \text{ g/L}$ ;  $[BA500] = 0.5 \text{ g/L}$ ;  $[PM500-EDTA-2 \text{ h}] = 0.5 \text{ g/L}$ ;  $[PM500-Glycerol-30 \text{ min}] = 0.5 \text{ g/L}$ ;  $T = 25 \text{ } ^\circ\text{C}$ ;  $\text{pH} = 7.4$  (20 mM PBS).

TC, but the catalytic ability of different biochar samples varied greatly. PM500 possesses the highest catalytic capacity, while PM500-EDTA-2 h has little effect on the activation of H<sub>2</sub>O<sub>2</sub>. The results of TOC measurement also provide a support to this conclusion. It can be observed that about 67% of organic pollutants were removed in PM500/H<sub>2</sub>O<sub>2</sub> system after 4 h reaction (Fig. S1), indicating the high removal efficiency of organics while only 13% of pollutants were adsorbed. Besides, there was no existence of metals observed in the remaining solution after degradation reaction indicating that metals bound tightly with other structures of biochar and would not cause secondary pollution through released from surface of biochar.

The stability of the catalyst is an important issue that should be considered before actual application, while reusability is a common indicator for evaluating the stability of materials. As shown in Fig. S2, four-cycle experiments were utilized to explore the reusability of biochar/H<sub>2</sub>O<sub>2</sub> systems for the removal of TC. It was found that three types of biochar all exhibited good reusability while PM500 performed best. Original PM500 could achieve the complete removal of TC in 3 h reaction, and it demonstrated great reusability by providing 98.2% TC removal efficiency in the 2nd run. Moreover, 86.3% and 74.5% of TC were removed in the 3rd and 4th runs, respectively. Many metal catalysts usually possessed poor reusability in spite of its high catalytic performance. In contrast, biochar with higher stability have more development potential.

### 3.3. Reactive species generated in biochar/H<sub>2</sub>O<sub>2</sub> systems

It has been well established that pollutants can be degraded by the radicals generated from the activation of H<sub>2</sub>O<sub>2</sub> in the Fenton/Fenton-like process. In order to further explore the reaction mechanism, the dominant radical that contributes to the degradation of TC was identified by free radical trapping experiments. In this paper, isopropyl alcohol (IPA) was utilized for hydroxyl radical ( $\cdot\text{OH}$ ) scavenger and 1,4-benzoquinone (BQ) was used for superoxide radical ( $\text{O}_2^{\cdot-}$ ) scavenger [13]. According to Fig. S3, addition of 5 mM BQ caused a slight decrease in the degradation rate of TC in three types of biochar/H<sub>2</sub>O<sub>2</sub> systems, indicating that  $\text{O}_2^{\cdot-}$  only had a little effect in SMT degradation. However, 5 mM IPA had a significant influence on the TC degradation since the degradation rate of TC in PM500/H<sub>2</sub>O<sub>2</sub> system decreased dramatically from 100% to 53.14% with the addition of IPA. Same tendency also can be found in other two systems. These phenomenon revealed that  $\cdot\text{OH}$  was the dominant radical in biochar/H<sub>2</sub>O<sub>2</sub> systems and played a key role in the catalytic process.

To further demonstrate that biochar have the ability to catalyze H<sub>2</sub>O<sub>2</sub>, the activation of H<sub>2</sub>O<sub>2</sub> with different biochar was studied by using EPR spectroscopy coupled with DMPO as a spin-trapping agent. This technique can detect the generation of  $\cdot\text{OH}$ , which are reportedly contributed to the degradation of contaminants in the Fenton-like system. According to Fig. 5a, 5 mM H<sub>2</sub>O<sub>2</sub> mixed with 0.2 M DMPO resulting in the formation of DMPO-OH signals (four lines, 1:2:2:1). These signals were identified from the hyperfine splitting constants (DMPO-OH:  $a_{\text{H}} = a_{\text{N}} = 15.03$  G) analyzed by EPRstudio software. The results suggested that there was a small quantity of  $\cdot\text{OH}$  generated in H<sub>2</sub>O<sub>2</sub> solution without biochar, and their peak intensities (DMPO-OH) were 964 au. However, after the addition of 0.5 g·L<sup>-1</sup> PM500, the peak intensities of DMPO-OH increased sharply to 5635 au, indicating that the addition of PM500 promoted the generation of  $\cdot\text{OH}$  in PM500/H<sub>2</sub>O<sub>2</sub> system. Moreover, there was no DMPO-OH signal observed in biochar suspensions without H<sub>2</sub>O<sub>2</sub>. These results suggested that PM500 can efficiently activate H<sub>2</sub>O<sub>2</sub> to produce  $\cdot\text{OH}$  and the other two biochar (BA500, CN500) have the similar ability. As shown in Fig. 5b, the intensity of DMPO-OH signals formed in the biochar/H<sub>2</sub>O<sub>2</sub> system followed this order: PM500 > CN500 > BA500.

The concentrations of  $\cdot\text{OH}$  and the activation ability of biochar in the biochar/H<sub>2</sub>O<sub>2</sub> system can be indicated by the peak intensities of DMPO-OH. As shown in Fig. 6a, the peak intensities of DMPO-OH with

different reaction time were determined. The results suggested that the peak intensities of DMPO-OH increased rapidly to 2144 au for BA500 within 5 min, to 3375 au for CN500 within 7 min and to 5562 au for PM500 within 10 min and remained steady as the reaction time extended to 30 min. According to Fig. 6b, the peak intensities of DMPO-OH in PM500-Glycerol-30 min/H<sub>2</sub>O<sub>2</sub> and PM500-EDTA-2 h/H<sub>2</sub>O<sub>2</sub> were much lower than in PM500/H<sub>2</sub>O<sub>2</sub>, which indicated that biochar produced from the biomass treated by Glycerol and EDTA was less reactive than biochar without treatment for H<sub>2</sub>O<sub>2</sub> activation. Moreover, it was found that there is a significant decrease in the concentration of PFRs in biochar after reaction with H<sub>2</sub>O<sub>2</sub> for 30 min (Fig. 6c), which revealed that the PFRs were consumed during the activation process.

### 3.4. Possible catalytic mechanism of biochar for H<sub>2</sub>O<sub>2</sub> activation

Results of correlation analysis (Text S1) among PFRs,  $\cdot\text{OH}$  generation, and TC degradation in biochar/H<sub>2</sub>O<sub>2</sub> systems demonstrated that PFRs play a key role in the process of activating H<sub>2</sub>O<sub>2</sub> by biochar to produce hydroxyl radicals for the degradation of tetracycline (Fig. S4). It has been well established that PFRs can transfer electron like electron shuttles. For instance, Dellinger found that the superoxide radical ion can be formed through electron transfer from PFRs existed in combustion products to molecular oxygen [65]. The redox ability of biochar also has been analyzed with electrochemical methods, and found that biochar can cause the electron transfer between iron oxide and bacteria [54,55]. Therefore, it was speculated that the catalytic mechanism of PFRs in biochar for H<sub>2</sub>O<sub>2</sub> activation may follow electron transfer pathways that can be described in Scheme 1. Subsequent experiment can be used to demonstrate this electron transfer mechanism. Many previous studies used K<sub>2</sub>Cr<sub>2</sub>O<sub>7</sub> to explore the electron transfer process in reaction system due to its efficient ability to remove electrons [66–68]. In this study, K<sub>2</sub>Cr<sub>2</sub>O<sub>7</sub> was used to investigate the catalytic mechanism of biochar for H<sub>2</sub>O<sub>2</sub> activation. According to Fig. 7a, peak intensities of DMPO-OH were significantly decreased with the addition of 5 mM K<sub>2</sub>Cr<sub>2</sub>O<sub>7</sub>, indicating that the formation of DMPO-OH was inhibited. Previous studies demonstrated that the reaction between DMPO-OH and K<sub>2</sub>Cr<sub>2</sub>O<sub>7</sub> can be ignored [69,70]. Hence, this result revealed that the generation of  $\cdot\text{OH}$  was greatly suppressed. As shown in Fig. 7b, the concentration of PFRs in biochar was markedly decreased from  $14.13 \times 10^{18}$  to  $4.37 \times 10^{18}$  spins·g<sup>-1</sup> for PM500,  $9.67 \times 10^{18}$  to  $3.39 \times 10^{18}$  spins·g<sup>-1</sup> for CN500, and  $7.94 \times 10^{18}$  to  $2.96 \times 10^{18}$  spins·g<sup>-1</sup> for BA500 with the addition of K<sub>2</sub>Cr<sub>2</sub>O<sub>7</sub>. These decrease degree were much greater than the decline tendency of the same systems where H<sub>2</sub>O<sub>2</sub> is existed, which indicated that K<sub>2</sub>Cr<sub>2</sub>O<sub>7</sub> possesses the stronger ability to capture electrons than H<sub>2</sub>O<sub>2</sub>. The reason for the suppressed generation of  $\cdot\text{OH}$  could be that the electron transfer pathway from PFRs to H<sub>2</sub>O<sub>2</sub> was cut off by K<sub>2</sub>Cr<sub>2</sub>O<sub>7</sub>. Therefore, the electron transfer pathway from PFRs to H<sub>2</sub>O<sub>2</sub> may be the catalytic mechanism of biochar for H<sub>2</sub>O<sub>2</sub> activation. Nonetheless, more studies should be conducted to further explore the possible reaction mechanism in biochar/H<sub>2</sub>O<sub>2</sub> systems.

Linear sweep voltammetry (LSV) (Text S2) was also conducted to explore the electron transfer process for the better elucidation of the proposed catalytic mechanism of biochar. It can be observed that there was tiny current response in the electrolyte containing H<sub>2</sub>O<sub>2</sub> when bar GCE acted as the working electrode (Fig. 8), which demonstrated that electron transfer at the GCE electrode interface was very slow. The reason for this phenomenon could be attributed to the high resistance of GCE electrode [20]. Compared with original GCE electrode, PM500-GCE possessed better electrical conductivity due to the bigger current response appeared in the electrolyte when PM500-GCE electrode existed alone. What is more, the current response in the electrolyte increased significantly with the addition of H<sub>2</sub>O<sub>2</sub> when PM500-GCE acted as the working electrode, revealing the enhanced reaction and rapid electron transfer between H<sub>2</sub>O<sub>2</sub> and PM500. The addition of TC also promoted this process which may be attributed to the consumption of

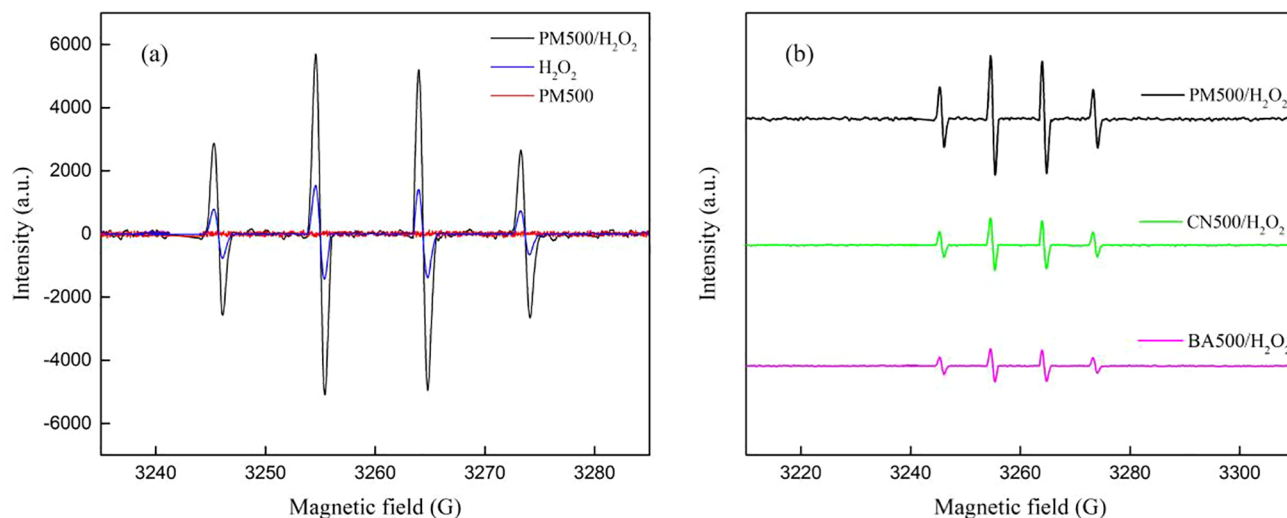


**Fig. 5.** EPR spectra of (a) PM500, H<sub>2</sub>O<sub>2</sub> and PM500/H<sub>2</sub>O<sub>2</sub> in the presence of DMPO at 30 min and (b) BA500/H<sub>2</sub>O<sub>2</sub>, CN500/H<sub>2</sub>O<sub>2</sub> and PM500/H<sub>2</sub>O<sub>2</sub> in the presence of DMPO at 30 min. Experimental conditions: [H<sub>2</sub>O<sub>2</sub>]<sub>0</sub> = 5 mM; [PM500] = 0.5 g/L; [CN500] = 0.5 g/L; [BA500] = 0.5 g/L; [DMPO]<sub>0</sub> = 0.2 M; T = 25 °C; pH = 7.4 (20 mM PBS).

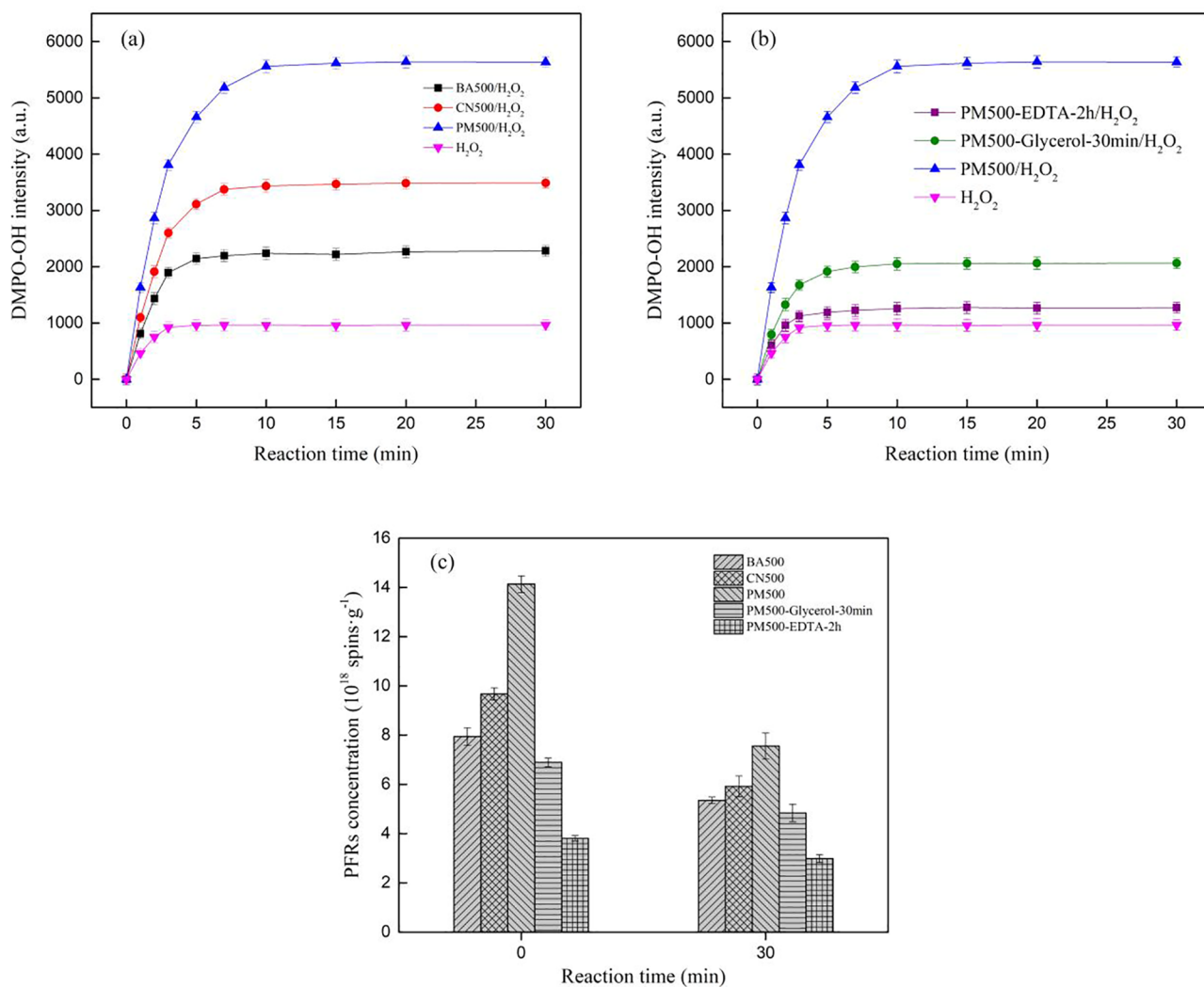


**Fig. 6.** Peak intensities of DMPO-OH in three types of biochar/H<sub>2</sub>O<sub>2</sub> systems (a) and in three pig manure biochar/H<sub>2</sub>O<sub>2</sub> systems (b); Changes of the concentration of PFRs in different biochar after reaction with H<sub>2</sub>O<sub>2</sub> for 30 min (c). Experimental conditions: [H<sub>2</sub>O<sub>2</sub>]<sub>0</sub> = 5 mM; [PM500] = 0.5 g/L; [CN500] = 0.5 g/L; [BA500] = 0.5 g/L; [PM500-EDTA-2 h] = 0.5 g/L; [PM500-Glycerol -30 min] = 0.5 g/L; [DMPO]<sub>0</sub> = 0.2 M; T = 25 °C; pH = 7.4 (20 mM PBS); the quality of biochar samples used in experiment was 20 mg.

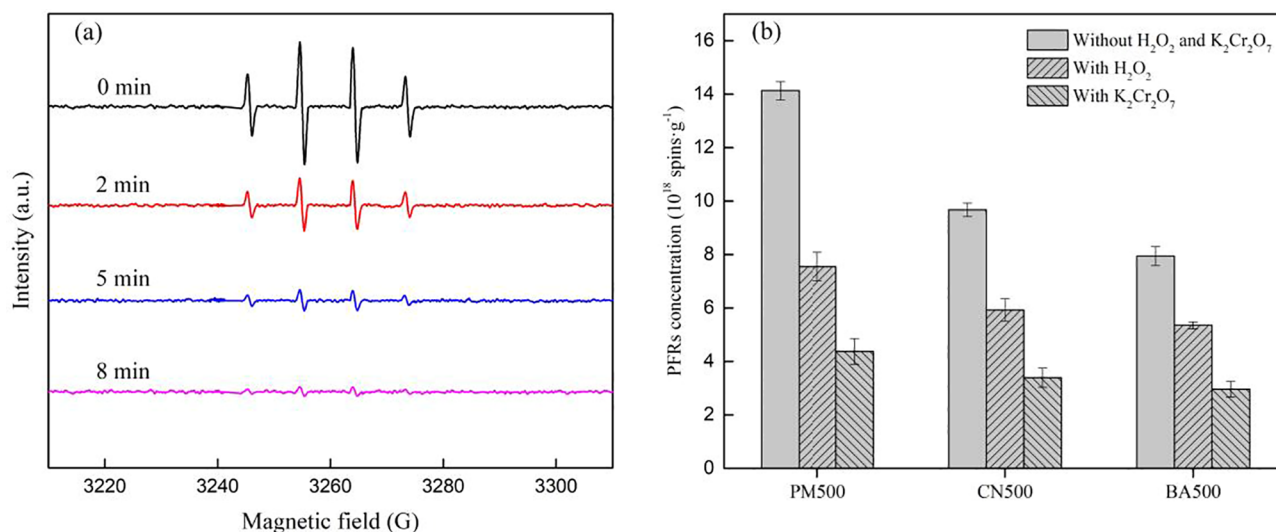


**Fig. 7.** Changes of the peak intensities of DMPO-OH formed in PM500/H<sub>2</sub>O<sub>2</sub> system with the existence of K<sub>2</sub>Cr<sub>2</sub>O<sub>7</sub> for different time (a); changes of PFRs concentration in three types of biochar with different reaction condition (b). Experimental conditions: [H<sub>2</sub>O<sub>2</sub>]<sub>0</sub> = 5 mM; [K<sub>2</sub>Cr<sub>2</sub>O<sub>7</sub>]<sub>0</sub> = 5 mM; [PM500] = 0.5 g/L; [CN500] = 0.5 g/L; [BA500] = 0.5 g/L; [DMPO]<sub>0</sub> = 0.2 M; T = 25 °C; pH = 7.4 (20 mM PBS); the quality of biochar samples used in experiment was 20 mg.

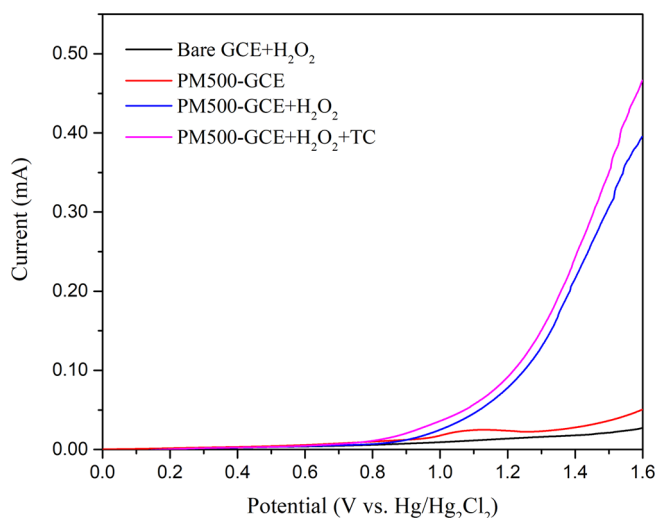


**Fig. 8.** Linear sweep voltammograms (LSV) obtained by the bare electrode (bare GCE) and PM500 electrode (PM500-GCE) in the presence of H<sub>2</sub>O<sub>2</sub> or TC, Experimental conditions: [H<sub>2</sub>O<sub>2</sub>]<sub>0</sub> = 5 mM; [PM500] = 0.5 g/L; [TC]<sub>0</sub> = 67.5 μM; T = 25 °C; pH = 7.4 (20 mM PBS).

reactive radical. These results provided a good support to the proposed catalytic mechanism of biochar.

### 3.5. Degradation intermediates and pathways of the TC

To fully understand the degradation process of TC in biochar/H<sub>2</sub>O<sub>2</sub> systems, LC-MS analyses (Text S3) were conducted to identify the oxidation products of TC in PM500/H<sub>2</sub>O<sub>2</sub> system. As shown in Fig. S5, MS spectra of the TC and its degradation intermediate at a different reaction time have been obtained. There were six main degradation intermediates of TC (*m/z* 445.2), which included TC 1 (*m/z* 461.2), TC 2 (*m/z* 362.6), TC 3 (*m/z* 416.5), TC 4 (*m/z* 398.3), TC 5 (*m/z* 225.1), and TC 6 (*m/z* 284.2). According to the detected intermediate products and the results of free radical trapping experiments, possible degradation pathways of TC were proposed and elucidated in Fig. 9. In general, TC molecular could be attacked by ·OH and O<sub>2</sub><sup>·-</sup>, while ·OH was the dominant reactive radicals. TC 1 was formed through the hydroxylation of TC molecular attacked by ·OH. Then, TC 2 could be produced as the

product ions through the rupture of carbon chain in the hydroxylated product (TC 1) [4]. TC 3 was formed through the detachments of N-methyl and amino group in TC molecular caused by O<sub>2</sub><sup>·-</sup> and it could further transform to TC 4 via dehydration reaction [71]. With the progressed reaction, TC 2 and TC 4 could be further oxidized and ring-opened, which led to the appearance of TC 5 and TC 6 [71]. These ring-opening products would finally be oxidized into CO<sub>2</sub> and H<sub>2</sub>O.

### 3.6. Effects of the TC adsorption on biochar/H<sub>2</sub>O<sub>2</sub> systems

The degradation and adsorption of TC were coexisted in biochar/H<sub>2</sub>O<sub>2</sub> systems. Therefore, it was necessary to study the interaction between the adsorption of TC and the catalytic reactivity of biochar toward H<sub>2</sub>O<sub>2</sub>. Before the addition of H<sub>2</sub>O<sub>2</sub>, biochar was used as an adsorbent to adsorb TC for different time. As expected in Fig. S6, both the degradation of TC and the DMPO-OH intensity were decreased significantly with the extended adsorption time. Previous work demonstrated that π-π electron-donor-acceptor interaction and other physical chemistry reaction processes occurred on the surface of chars during TC adsorption [44]. TC molecules that adsorbed to the surface of biochar and entered into the pore structure of biochar may cause the inactivation of surface reactivity and the blocking of the pore, which could weaken the electrons transfer ability of biochar and decrease the active sites on the surface of biochar. Thus, the accessibility of H<sub>2</sub>O<sub>2</sub> to biochar was impeded as the adsorption time extended, leading to the inhibited degradation of TC.

### 3.7. Real wastewater application

It is necessary to explore the application of biochar/H<sub>2</sub>O<sub>2</sub> systems in real wastewater. The composition of actual wastewater is extremely complex compared to ultrapure water. Thus, there were great differences existed in pollutant removal efficiencies between simulated wastewater and actual polluted wastewater. For this purpose, the degradation of TC in PM500/H<sub>2</sub>O<sub>2</sub> system with four types of water was studied, which included ultrapure water, tap water (Waterworks, Changsha), river water (Xiangjiang River, Changsha), and municipal wastewater (Changsha 3rd sewage treatment plant, China). As shown in Fig. S7, the TC removal efficiencies in PM500/H<sub>2</sub>O<sub>2</sub> system with different water within 4 h were 100% for ultrapure water, 100% for tap water, 95.4% for river water, and 83.7% for municipal wastewater, respectively. Tap water produced from waterworks in Changsha was



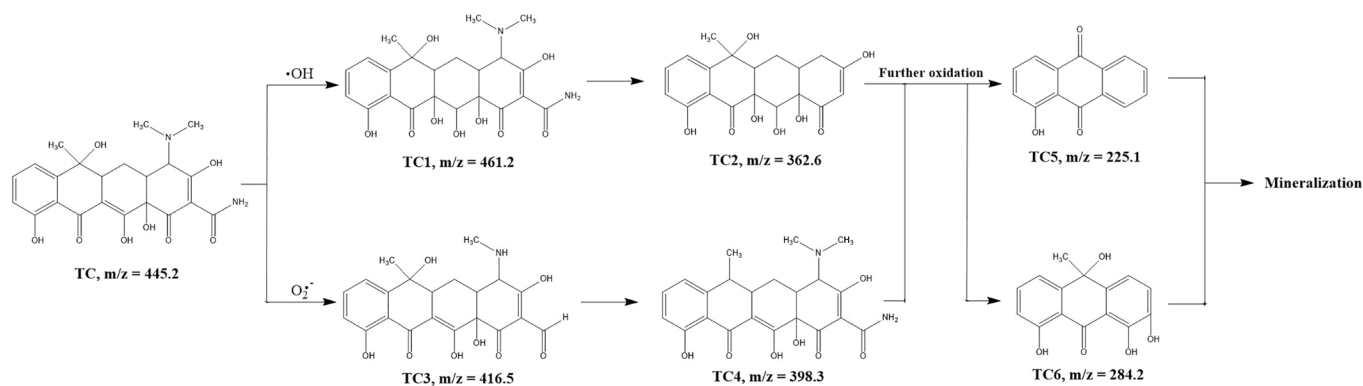


Fig. 9. Suggested degradation pathways of TC in PM500/H<sub>2</sub>O<sub>2</sub> system.

sterilized by chlorine, which would generate free residual chlorine (ClO<sup>-</sup>, HClO, and Cl<sub>2</sub>, etc.) with strong oxidizing property. The tap water used in this study was detected by residual chlorine comparator (CL1600, China), and found that there was about 0.02 mg/L free residual chlorine in this water (Table S3). These free residual chlorines still have a slight inhibition on the TC degradation rates in PM500/H<sub>2</sub>O<sub>2</sub> systems in spite of its small quantities (Fig. S7). As present in Table S3, The river water contained small amounts of metals and nitrogen and phosphorus organic compounds while there were abundant organic matters existed in municipal wastewater. All of these components would be adsorbed on the surface of PM500 in the activation process of H<sub>2</sub>O<sub>2</sub> by PM500 [27,72]. The results of real wastewater application experiments suggested that the TC degradation rates decreased lightly in river water while there was a remarkable decrease of the TC degradation rates observed in municipal wastewater (Fig. S7). This phenomenon revealed that PM500 possessed good stability which adsorption of a small amount of other pollutants has little effect on the catalytic capacity of PM500. However, high amounts of organic pollutants coexisted in the environment would cover the active site of PM500 through adsorption and could even compete with TC for ·OH, causing the lower removal of TC in municipal wastewater. These results indicated that PM500/H<sub>2</sub>O<sub>2</sub> system possessed a great potential for practical treatment of real wastewater and exhibited good versatility which can efficiently work in complicated condition.

#### 4. Conclusions

In summary, three types of biochar (PM500, CN500, and BA500) possessed good stability and exhibited excellent catalytic ability to activate H<sub>2</sub>O<sub>2</sub> so that it can produce ·OH to efficiently degrade TC. It was found that PFRs played an essential role in the catalytic performance of biochar. Biochar with higher concentration of PFRs had more active reactivity, while the more amounts of PFRs consumed during the reaction, the more amounts of ·OH generated in biochar/H<sub>2</sub>O<sub>2</sub> systems. The possible catalytic mechanism of biochar was the electrons transfer pathways from PFRs to H<sub>2</sub>O<sub>2</sub>. The adsorption of TC on biochar could hinder the active site of the reaction between PFRs and H<sub>2</sub>O<sub>2</sub> so that the degradation of TC was suppressed in biochar/H<sub>2</sub>O<sub>2</sub> systems. Similar phenomenon was also observed in real wastewater application. Additionally, the results indicated that the concentrations of PFRs in biochar markedly decreased with the reduction of the content of phenolic compounds (e.g., phenol, chlorophenol) and metals (e.g., Ca, Mg, Cu, Fe, and Zn) in the feedstock, and the influence of metals on the formation of PFRs was greater than phenolic compounds. It was inferred that metals, like a central skeleton, can connect the parts of PFRs by chemical bonds, while phenolic compounds or specific organic compounds may constitute the PFRs and its amount can determine the concentration of PFRs. Therefore, the difference of the components of phenolic compounds and metals in biomass can affect the amount of

PFRs formed in biochar that pyrolysed from these biomasses and have a great influence on the catalytic ability of biochar for H<sub>2</sub>O<sub>2</sub> activation. The biomass with more appropriate organic and metal ratios may produce biochar with better catalytic properties. The findings of this study make a better interpretation about the formation mechanism of PFRs in biochar and provide a new insight into the selection of feedstock that can produce more efficient biochar. In addition, specific function of single metal elements on the formation of PFRs in biochar and the most suitable ratio of organic compounds and metals in biomass will require further study in the future.

#### 5. A Competing interest statement

We declared that we have no competing interests.

#### Acknowledgments

This study was financially supported by the Program for the National Natural Science Foundation of China (51879101, 51579098, 51779090, 51709101, 51521006, 51809090, 51278176, 51378190), the National Program for Support of Top-Notch Young Professionals of China (2014), the Program for Changjiang Scholars and Innovative Research Team in University (IRT-13R17), and Hunan Provincial Science and Technology Plan Project (2018SK20410, 2017SK2243, 2016RS3026), and the Fundamental Research Funds for the Central Universities (531109200027, 531107051080, 531107050978).

#### Appendix A. Supplementary data

Supplementary data to this article can be found online at <https://doi.org/10.1016/j.cej.2018.12.098>.

#### References

- [1] D.L. Huang, C.J. Hu, G.M. Zeng, M. Cheng, P.A. Xu, X.M. Gong, R.Z. Wang, W.J. Xue, Combination of Fenton processes and biotreatment for wastewater treatment and soil remediation, *Sci. Total Environ.* 574 (2017) 1599–1610.
- [2] K.E. O'Shea, D.D. Dionysiou, Advanced oxidation processes for water treatment, *J. Phys. Chem. Lett.* 3 (2012) 2112–2113.
- [3] A.A. Burbano, D.D. Dionysiou, M.T. Suidan, T.L. Richardson, Oxidation kinetics and effect of pH on the degradation of MTBE with Fenton reagent, *Water Res.* 39 (2005) 107–118.
- [4] M. Cheng, G. Zeng, D. Huang, C. Lai, P. Xu, C. Zhang, Y. Liu, Hydroxyl radicals based advanced oxidation processes (AOPs) for remediation of soils contaminated with organic compounds: a review, *Chem. Eng. J.* 284 (2016) 582–598.
- [5] E. Neyens, J. Baeyens, A review of classic Fenton's peroxidation as an advanced oxidation technique, *J. Hazard. Mater.* 98 (2003) 33–50.
- [6] G.P. Anipsitakis, D.D. Dionysiou, Radical generation by the interaction of transition metals with common oxidants, *Environ. Sci. Technol.* 38 (2004) 3705–3712.
- [7] D. Huang, W. Xue, G. Zeng, J. Wan, G. Chen, C. Huang, C. Zhang, M. Cheng, P. Xu, Immobilization of Cd in river sediments by sodium alginate modified nanoscale zero-valent iron: impact on enzyme activities and microbial community diversity, *Water Res.* 106 (2016) 15–25.
- [8] D. Huang, Z. Hu, Z. Peng, G. Zeng, G. Chen, C. Zhang, M. Cheng, J. Wan, X. Wang,

- X. Qin, Cadmium immobilization in river sediment using stabilized nanoscale zero-valent iron with enhanced transport by polysaccharide coating, *J. Environ. Manage.* 210 (2018) 191–200.
- [9] C. Hu, D. Huang, G. Zeng, M. Cheng, X. Gong, R. Wang, W. Xue, Z. Hu, Y. Liu, The combination of Fenton process and *Phanerochaete chrysosporium* for the removal of bisphenol A in river sediments: mechanism related to extracellular enzyme, organic acid and iron, *Chem. Eng. J.* 338 (2018) 432–439.
- [10] G.P. Anipsitakis, D.D. Dionysiou, Degradation of organic contaminants in water with sulfate radicals generated by the conjunction of peroxymonosulfate with cobalt, *Environ. Sci. Technol.* 37 (2003) 4790–4797.
- [11] G.P. Anipsitakis, D.D. Dionysiou, Transition metal/UV-based advanced oxidation technologies for water decontamination, *Appl. Catal. B* 54 (2004) 155–163.
- [12] D.-L. Huang, R.-Z. Wang, Y.-G. Liu, G.-M. Zeng, C. Lai, P. Xu, B.-A. Lu, J.-J. Xu, C. Wang, C. Huang, Application of molecularly imprinted polymers in wastewater treatment: a review, *Environ. Sci. Pollut. R* 22 (2015) 963–977.
- [13] M. Cheng, G. Zeng, D. Huang, C. Lai, Y. Liu, C. Zhang, J. Wan, L. Hu, C. Zhou, W. Xiong, Efficient degradation of sulfamethazine in simulated and real wastewater at slightly basic pH values using Co-SAM-SCS/H<sub>2</sub>O<sub>2</sub> Fenton-like system, *Water Res.* 138 (2018) 7–18.
- [14] Y. Wang, X. Shen, F. Chen, Improving the catalytic activity of CeO<sub>2</sub>/H<sub>2</sub>O<sub>2</sub> system by sulfation pretreatment of CeO<sub>2</sub>, *J. Mol. Catal. A: Chem.* 381 (2014) 38–45.
- [15] F. Chen, X. Shen, Y. Wang, J. Zhang, CeO<sub>2</sub>/H<sub>2</sub>O<sub>2</sub> system catalytic oxidation mechanism study via a kinetics investigation to the degradation of acid orange 7, *Appl. Catal. B* 121 (2012) 223–229.
- [16] N.H. Ince, I.G. Apikyan, Combination of activated carbon adsorption with light-enhanced chemical oxidation via hydrogen peroxide, *Water Res.* 34 (2000) 4169–4176.
- [17] F. Rodriguez-Reinos, The role of carbon materials in heterogeneous catalysis, *Carbon* 36 (1998) 159–175.
- [18] P. Serp, J.L. Figueredo, *Carbon materials for catalysis*, first ed., John Wiley & Sons, New Jersey, 2008.
- [19] C. Gomez, A. Silva, M. Strumia, L. Avale, M. Rojas, The origin of high electrocatalytic activity of hydrogen peroxide reduction reaction by a gC<sub>3</sub>N<sub>4</sub>/HOPG sensor, *Nanoscale* 9 (2017) 11170–11179.
- [20] L. Tang, Y. Liu, J. Wang, G. Zeng, Y. Deng, H. Dong, H. Feng, J. Wang, B. Peng, Enhanced activation process of persulfate by mesoporous carbon for degradation of aqueous organic pollutants: electron transfer mechanism, *Appl. Catal. B* 231 (2018) 1–10.
- [21] F. Zhou, C. Lu, Y. Yao, L. Sun, F. Gong, D. Li, K. Pei, W. Lu, W. Chen, Activated carbon fibers as an effective metal-free catalyst for peracetic acid activation: implications for the removal of organic pollutants, *Chem. Eng. J.* 281 (2015) 953–960.
- [22] D.D. Dionysiou, Environmental applications and implications of nanotechnology and nanomaterials, *J. Environ. Eng.* 130 (2004) 723–724.
- [23] G. Fang, J. Gao, D.D. Dionysiou, C. Liu, D. Zhou, Activation of persulfate by quinones: free radical reactions and implication for the degradation of PCBs, *Environ. Sci. Technol.* 47 (2013) 4605–4611.
- [24] E. Marris, Putting the carbon back: Black is the new green, *Nature* 442 (2006) 624–626.
- [25] D. Huang, L. Liu, G. Zeng, P. Xu, C. Huang, L. Deng, R. Wang, J. Wan, The effects of rice straw biochar on indigenous microbial community and enzymes activity in heavy metal-contaminated sediment, *Chemosphere* 174 (2017) 545–553.
- [26] D. Huang, R. Deng, J. Wan, G. Zeng, W. Xue, X. Wen, C. Zhou, L. Hu, X. Liu, P. Xu, Remediation of lead-contaminated sediment by biochar-supported nano-chlorapatite: Accompanied with the change of available phosphorus and organic matters, *J. Hazard. Mater.* 348 (2018) 109–116.
- [27] R.-Z. Wang, D.-L. Huang, Y.-G. Liu, C. Zhang, C. Lai, G.-M. Zeng, M. Cheng, X.-M. Gong, J. Wan, H. Luo, Investigating the adsorption behavior and the relative distribution of Cd<sup>2+</sup> sorption mechanisms on biochars by different feedstock, *Bioresour. Technol.* 261 (2018) 265–271.
- [28] D. Huang, X. Wang, C. Zhang, G. Zeng, Z. Peng, J. Zhou, M. Cheng, R. Wang, Z. Hu, X. Qin, Sorptive removal of ionizable antibiotic sulfamethazine from aqueous solution by graphene oxide-coated biochar nanocomposites: influencing factors and mechanism, *Chemosphere* 186 (2017) 414–421.
- [29] G. Fang, J. Gao, C. Liu, D.D. Dionysiou, Y. Wang, D. Zhou, Key role of persistent free radicals in hydrogen peroxide activation by biochar: implications to organic contaminant degradation, *Environ. Sci. Technol.* 48 (2014) 1902–1910.
- [30] G. Fang, C. Liu, J. Gao, D.D. Dionysiou, D. Zhou, Manipulation of persistent free radicals in biochar to activate persulfate for contaminant degradation, *Environ. Sci. Technol.* 49 (2015) 5645–5653.
- [31] J.J. Pignatello, W.A. Mitch, W. Xu, Activity and reactivity of pyrogenic carbonaceous matter toward organic compounds, *Environ. Sci. Technol.* 51 (2017) 8893–8908.
- [32] D. Huang, X. Guo, Z. Peng, G. Zeng, P. Xu, X. Gong, R. Deng, W. Xue, R. Wang, H. Yi, White rot fungi and advanced combined biotechnology with nanomaterials: promising tools for endocrine-disrupting compounds biotransformation, *Crit. Rev. Biotechnol.* 38 (2018) 671–689.
- [33] D. Huang, Z. Tang, Z. Peng, C. Lai, G. Zeng, C. Zhang, P. Xu, M. Cheng, J. Wan, R. Wang, Fabrication of water-compatible molecularly imprinted polymer based on  $\beta$ -cyclodextrin modified magnetic chitosan and its application for selective removal of bisphenol A from aqueous solution, *J. Taiwan. Inst. Chem. E* 77 (2017) 113–121.
- [34] J. Yang, J.J. Pignatello, B. Pan, B. Xing, Degradation of p-nitrophenol by lignin and cellulose chars: H<sub>2</sub>O<sub>2</sub>-mediated reaction and direct reaction with the char, *Environ. Sci. Technol.* 51 (2017) 8972–8980.
- [35] X. Gong, D. Huang, Y. Liu, Z. Peng, G. Zeng, P. Xu, M. Cheng, R. Wang, J. Wan, Remediation of contaminated soils by biotechnology with nanomaterials: bio-behavior, applications, and perspectives, *Crit. Rev. Biotechnol.* 38 (2018) 455–468.
- [36] D. Huang, Y. Wang, C. Zhang, G. Zeng, C. Lai, J. Wan, L. Qin, Y. Zeng, Influence of morphological and chemical features of biochar on hydrogen peroxide activation: implications on sulfamethazine degradation, *RSC Adv.* 6 (2016) 73186–73196.
- [37] S. Lomnicki, H. Truong, E. Vejerano, B. Dellinger, Copper oxide-based model of persistent free radical formation on combustion-derived particulate matter, *Environ. Sci. Technol.* 42 (2008) 4982–4988.
- [38] E. Vejerano, S. Lomnicki, B. Dellinger, Formation and stabilization of combustion-generated environmentally persistent free radicals on an Fe(III)<sub>2</sub>O<sub>3</sub>/silica surface, *Environ. Sci. Technol.* 45 (2010) 589–594.
- [39] E. Vejerano, S. Lomnicki, B. Dellinger, Lifetime of combustion-generated environmentally persistent free radicals on Zn(II)O and other transition metal oxides, *J. Environ. Monit.* 14 (2012) 2803–2806.
- [40] E. Vejerano, S.M. Lomnicki, B. Dellinger, Formation and stabilization of combustion-generated, environmentally persistent radicals on Ni(II)O supported on a silica surface, *Environ. Sci. Technol.* 46 (2012) 9406–9411.
- [41] Y. Sun, B. Gao, Y. Yao, J. Fang, M. Zhang, Y. Zhou, H. Chen, L. Yang, Effects of feedstock type, production method, and pyrolysis temperature on biochar and hydrochar properties, *Chem. Eng. J.* 240 (2014) 574–578.
- [42] H. Zhang, C. Chen, E.M. Gray, S.E. Boyd, Effect of feedstock and pyrolysis temperature on properties of biochar governing end use efficacy, *Biomass Bioenergy* 105 (2017) 136–146.
- [43] X. Gong, D. Huang, Y. Liu, G. Zeng, R. Wang, J. Wei, C. Huang, P. Xu, J. Wan, C. Zhang, Pyrolysis and reutilization of plant residues after phytoremediation of heavy metals contaminated sediments: for heavy metals stabilization and dye adsorption, *Bioresour. Technol.* 253 (2018) 64–71.
- [44] C. Zhang, C. Lai, G. Zeng, D. Huang, C. Yang, Y. Wang, Y. Zhou, M. Cheng, Efficacy of carbonaceous nanocomposites for sorbing ionizable antibiotic sulfamethazine from aqueous solution, *Water Res.* 95 (2016) 103–112.
- [45] D. Wang, F. Jia, H. Wang, F. Chen, Y. Fang, W. Dong, G. Zeng, X. Li, Q. Yang, X. Yuan, Simultaneously efficient adsorption and photocatalytic degradation of tetracycline by Fe-based MOFs, *J. Colloid Interface Sci.* 519 (2018) 273–284.
- [46] Z. Xie, Y. Feng, F. Wang, D. Chen, Q. Zhang, Y. Zeng, W. Lv, G. Liu, Construction of carbon dots modified MoO<sub>3</sub>/g-C<sub>3</sub>N<sub>4</sub> Z-scheme photocatalyst with enhanced visible-light photocatalytic activity for the degradation of tetracycline, *Appl. Catal. B* 229 (2018) 96–104.
- [47] E. Fernández, R. Jiménez, A.M. Lallena, J. Aguilar, Evaluation of the BCR sequential extraction procedure applied for two unpolluted Spanish soils, *Environ. Pollut.* 131 (2004) 355–364.
- [48] X.L. Gao, W. Gang Chentung, Q.Z. Xue, T. Cheng, S.Y. Chen, Z.Y. Chen, T. Yanagi, E. Wolanski, Environmental status of Daya Bay surface sediments inferred from a sequential extraction technique, *Estuar. Coast. Shelf S* 86 (2010) 369–378.
- [49] C.-J.G. Pan, D.A. Schmitz, A.K. Cho, J. Froines, J.M. Fukuto, Inherent redox properties of diesel exhaust particles: catalysis of the generation of reactive oxygen species by biological reductants, *Toxicol. Sci.* 81 (2004) 225–232.
- [50] B.A. Smith, A.L. Teel, R.J. Watts, Identification of the reactive oxygen species responsible for carbon tetrachloride degradation in modified Fenton's systems, *Environ. Sci. Technol.* 38 (2004) 5465–5469.
- [51] A.L.N.d. Cruz, R.L. Cook, S.M. Lomnicki, B. Dellinger, Effect of low temperature thermal treatment on soils contaminated with pentachlorophenol and environmentally persistent free radicals, *Environ. Sci. Technol.* 46 (2012) 5971–5978.
- [52] Z. Maskos, B. Dellinger, Formation of the secondary radicals from the aging of tobacco smoke, *Energy Fuel* 22 (2007) 382–388.
- [53] Z. Maskos, B. Dellinger, Radicals from the oxidative pyrolysis of tobacco, *Energy Fuel* 22 (2008) 1675–1679.
- [54] A. Kappler, M.L. Wuestner, A. Ruecker, J. Harter, M. Halama, S. Behrens, Biochar as an electron shuttle between bacteria and Fe (III) minerals, *Environ. Sci. Technol. Lett.* 1 (2014) 339–344.
- [55] L. Klüpfel, M. Keilueit, M. Kleber, M. Sander, Redox properties of plant biomass-derived black carbon (biochar), *Environ. Sci. Technol.* 48 (2014) 5601–5611.
- [56] Y. Xu, Z. Lou, P. Yi, J. Chen, X. Ma, Y. Wang, M. Li, W. Chen, Q. Liu, J. Zhou, Improving abiotic reducing ability of hydrothermal biochar by low temperature oxidation under air, *Bioresour. Technol.* 172 (2014) 212–218.
- [57] L. Tian, C.P. Koshland, J. Yano, V.K. Yachandra, I.T. Yu, S. Lee, D. Lucas, Carbon-centered free radicals in particulate matter emissions from wood and coal combustion, *Energy Fuel* 23 (2009) 2523–2526.
- [58] T.C. Lo, M.H. Baird, C. Hanson, *Handbook of Solvent Extraction*, Wiley, New York etc, 1983.
- [59] W. Wu, M. Yang, Q. Feng, K. McGrouther, H. Wang, H. Lu, Y. Chen, Chemical characterization of rice straw-derived biochar for soil amendment, *Biomass Bioenergy* 47 (2012) 268–276.
- [60] X. Zhao, W. Ouyang, F. Hao, C. Lin, F. Wang, S. Han, X. Geng, Properties comparison of biochars from corn straw with different pretreatment and sorption behaviour of atrazine, *Bioresour. Technol.* 147 (2013) 338–344.
- [61] F. Czechowski, A. Jezierski, EPR studies on petrographic constituents of bituminous coals, chars of brown coals group components, and humic acids 600°C char upon oxygen and solvent action, *Energy Fuel* 11 (1997) 951–964.
- [62] P. Meshram, B.K. Purohit, M.K. Sinha, S. Sahu, B. Pandey, Demineralization of low grade coal—a review, *Renewable Sustainable Energy Rev.* 41 (2015) 745–761.
- [63] A. Ohki, T. Nakajima, H. Yamashita, A. Iwashita, H. Takanashi, Leaching of various metals from coal into aqueous solutions containing an acid or a chelating agent, *Fuel Process. Technol.* 85 (2004) 1089–1102.
- [64] B. Sun, F. Zhao, E. Lombi, S. McGrath, Leaching of heavy metals from contaminated soils using EDTA, *Environ. Pollut.* 113 (2001) 111–120.
- [65] B. Dellinger, S. Lomnicki, L. Khachatryan, Z. Maskos, R.W. Hall, J. Adoukpe, C. McFerrin, H. Truong, Formation and stabilization of persistent free radicals, *P. Combust. Inst.* 31 (2007) 521–528.

- [66] Y. Chen, S. Yang, K. Wang, L. Lou, Role of primary active species and TiO<sub>2</sub> surface characteristic in UV-illuminated photodegradation of Acid Orange 7, *J. Photochem. Photobiol. A: Chem.* 172 (2005) 47–54.
- [67] H. Fang, Y. Gao, G. Li, J. An, P.-K. Wong, H. Fu, S. Yao, X. Nie, T. An, Advanced oxidation kinetics and mechanism of preservative propylparaben degradation in aqueous suspension of TiO<sub>2</sub> and risk assessment of its degradation products, *Environ. Sci. Technol.* 47 (2013) 2704–2712.
- [68] X. Gong, D. Huang, Y. Liu, G. Zeng, R. Wang, J. Wan, C. Zhang, M. Cheng, X. Qin, W. Xue, Stabilized nanoscale zerovalent iron mediated cadmium accumulation and oxidative damage of *Boehmeria nivea* (L.) gaudich cultivated in cadmium contaminated sediments, *Environ. Sci. Technol.* 51 (2017) 11308–11316.
- [69] X. Guo, Z. Peng, D. Huang, P. Xu, G. Zeng, S. Zhou, X. Gong, M. Cheng, R. Deng, H. Yi, Biotransformation of cadmium-sulfamethazine combined pollutant in aqueous environments: phanerochaete chrysosporium bring cautious optimism, *Chem. Eng. J.* 347 (2018) 74–83.
- [70] X. Shi, N. Dalal, Evidence for a Fenton-type mechanism for the generation of OH radicals in the reduction of Cr (VI) in cellular media, *Arch. Biochem. Biophys.* 281 (1990) 90–95.
- [71] Z. Zhu, Y. Yu, H. Huang, X. Yao, H. Dong, Z. Liu, Y. Yan, C. Li, P. Huo, Microwave-hydrothermal synthesis of a novel, recyclable and stable photocatalytic nanoreactor for recognition and degradation of tetracycline, *Catal. Sci. Technol.* 7 (2017) 4092–4104.
- [72] Z. Peng, H. Sun, Y. Li, T. Sun, Adsorption and catalytic hydrolysis of carbaryl and atrazine on pig manure-derived biochars: impact of structural properties of biochars, *J. Hazard. Mater.* 244–245 (2013) 217–224.